Journal of Power Sources 185 (2008) 589–594

Contents lists available at ScienceDirect

Journal of Power Sources

journal homepage: www.elsevier.com/locate/jpowsour

The porous structures of activated carbon aerogels and their effects on electrochemical performance

Junbing Wang[a], Xiaoqing Yang[a], Dingcai Wu[a,b], Ruowen Fu[a,b,*], Mildred S. Dresselhaus[c], Gene Dresselhaus[c]

[a] Materials Science Institute, PCFM Laboratory, School of Chemistry and Chemical Engineering, Sun Yat-sen University, Guangzhou 510275, PR China
[b] Institute of Optoelectronic and Functional Composite Materials, Sun Yat-sen University, Guangzhou 510275, PR China
[c] Massachusetts Institute of Technology, 77 Massachusetts Avenue, Cambridge, MA 02139, USA

ARTICLE INFO

Article history:
Received 5 March 2008
Received in revised form 20 May 2008
Accepted 30 June 2008
Available online 6 July 2008

Keywords:
Carbon aerogel
Activation
Porosity
Electrochemical properties

ABSTRACT

The pore structures of carbon aerogels were designed and controlled by changing conditions for both the microemulsion-templated sol–gel polymerization and the KOH activation processes. The resulting pore structures were characterized by means of N_2 adsorption and SEM. A new pore model is proposed and the relationship between the pore structures of the activated carbon aerogels (ACAs) and their electrochemical performance is discussed. The experimental results show that the ACAs which were prepared contain four types of pores: (A) micropores with diameters below 2 nm; (B) small mesopores with diameters from 2 to 5 nm; (C) large mesopores with diameters from 5 to 40 nm; and (D) large pores and channels with diameters over 40 nm. Appropriate activation with KOH can increase the numbers of micropores and small mesopores as well as the BET areas, resulting in an increase in the specific capacitance (C_s) of the ACA samples. The type D pores and channels play an important role in the enhancement of the electrochemical capacitance under high charge–discharge current conditions. Though ACAs with different porous models show a linear relation between C_s and BET area separately, the surface areas of micropores of the ACAs with appropriate type D pores and channels have a higher accessibility and efficiency in the storage of energy than those with closed type C pores.

1. Introduction

Increasing attention has been paid to electrochemical capacitors because they provide a relatively safe and environmentally friendly electrical energy storage device. Porous carbon materials such as activated carbons, carbon aerogels, carbon xerogels, nanostructured carbons are usually utilized as electrode materials, and exhibit good electrochemical performance because these materials possess both a high surface area and pores which are adapted to the size of ions. These characteristics are crucial for good supercapacitor performance [1]. Carbon aerogels (CAs) are considered to be perfect electrode materials for electrochemical capacitors due to their unique three-dimensional nano-network, high specific surface area, abundant mesopores and high electric conductivity [2–4]. According to reports in the literature, it can be concluded that many factors affect the electrochemical performance of supercapacitors, including their specific surface area, pore volume, pore size distribution, as well as the surface groups of the electrode materials [4–8]. Meng et al. reported that both the surface area and pore volume of carbon aerogels determine their specific capacitance. High pore volume and wide pore distribution contribute to increasing their capacitance [5]. Frackowiak concluded that micropores (with diameters less than 2 nm) play an essential adsorption role in the formation of the electrical double layer, and the presence of mesopores (diameters 2–50 nm) is necessary for efficient charge propagation into the bulk of the electrode material, allowing the so-called frequency response to be fulfilled [6]. Azais et al. indicated that the concentration of surface groups and their nature were found to have an important influence on the performance degradation of supercapacitors [7]. Zhuang et al. reported that activated carbons with larger micropores have a larger specific capacitance and a higher discharge rate [8]. Summarizing the reported results in the literature, it was found that the electrochemical capacitance is generally proportional to the specific surface area for the same kind of carbon materials, but this relation is not necessarily valid when comparing different kinds of carbon materials. This is implied by observation that the energy storage efficiencies of the surface area for different carbons

* Corresponding author at: Materials Science Institute, PCFM Laboratory, School of Chemistry and Chemical Engineering, Sun Yat-sen University, Guangzhou 510275, PR China. Tel.: +86 20 84114527; fax: +86 20 84115112.
E-mail address: cesfrw@mail.sysu.edu.cn (R. Fu).

0378-7753/$ – see front matter © 2008 Elsevier B.V. All rights reserved.
doi:10.1016/j.jpowsour.2008.06.070

are not the same. From previous studies, we discovered that the CAs prepared under different conditions possess a variety of electrochemical capacitances and a range of dynamic charge–discharge performance. Up to now, the relationship between the porous structures of CAs and their electrochemical performance is not very clear. Therefore, the objective of the present research was to explore the relationship between the average pore size and the pore size distribution of CAs and their electrochemical performance. In this work, the pore structures of CAs were designed and controlled by changing the conditions under which the microemulsion-templated sol–gel polymerization and the subsequent activation were carried out. The pore structures of the samples and their electrochemical performance were studied by means of N_2 adsorption, cyclic voltammetric measurements, and other techniques.

2. Experimental

2.1. Preparation of CAs and activated carbon aerogels

The resorcinol-formaldehyde (RF) CAs were prepared by an ambient pressure drying method according to the procedure reported in the literature [9]. According to the predetermined formulations, all reactants, including resorcinol (R), formaldehyde (F), deionized water (W) and cetyltrimethylammonium bromide (C), were mixed by a magnetic stirrer and then transferred into a glass vial (~20 ml). The vial was sealed and then was put into a water bath (85 °C) to cure for 5 days. After curing, the gels were directly dried in air at room temperature for 2 days at first, and then further dried under an infrared lamp with an irradiation temperature of about 50 °C for 1 day, and finally dried in an oven at 110 °C at ambient pressure for 3 h. Subsequently, the resultant RF aerogels were pyrolyzed at 300–900 °C for 3 h in flowing N_2.

Activated carbon aerogels (ACAs) were prepared according to the following procedures: Approximately 2 g of CAs were mixed with KOH pellets at a mass ratio of KOH to CAs (K/CA ratio) ranging from 0.5/1 to 7/1 in a glass beaker and 5 ml ethanol was added to dissolve the KOH pellets. The mixture was dried at 110 °C and then carbonized in a tubular furnace at 900 °C for 3 h with a heating rate of 5 °C/min under flowing nitrogen. After the mixture cooled down to room temperature, the resultant materials were taken out and washed with 10% HCl and distilled water. Finally, the materials were dried at 110 °C for 6 h. The resulting products are referred to in the paper as ACA-*xx*/*yy*-K*z*, where the *xx*, *yy* and *z* denote the ratio of resorcinol to catalyst (R/C ratio), carbonization temperature, and the K/CA ratio, respectively. The activation yields of ACA samples are 16–68 wt% (e.g., for the ACA-500/500-K*z* series, when *z* = 1, 3, 5 and 7, and the yield = 63, 33, 27 and 16 wt%, respectively).

2.2. Measurement of the pore parameters

Samples of approximately 0.1 g were heated to 250 °C to remove all the adsorbed species. Nitrogen adsorption and desorption isotherms were then taken using an ASAP 2010 Surface Area Analyzer (Micromeritics Instrument Corporation). The BET surface area (S_{BET}), the micropore size distribution, the volume (V_{mic}) and surface area (S_{mic}) of micropore, and the volume (V_{mes}) and pore size distribution of mesopore were analyzed by BET (Brunauer-Emmett-Teller) theory, HK (Horvath-Kawazoe) theory, t-plot theory, and BJH (Barrett-Joyner-Halendar) theory, respectively.

2.3. SEM observation

The samples were mounted on a sample holder and coated with an Au alloy. The morphology images of the samples were recorded using a JEOL JSM-6330F Scanning Electron Microscope.

2.4. Electrochemical measurements

Measurement samples were prepared by mixing CA samples (with diameters less than 125 micron) and polytetrafluorethylene (PTFE) together in a ratio of 92:8, and then rolling the mixture into a film with a roller, cutting the film into a suitable shape and covering a 1 cm by 1 cm plain nickel foam (current collector) with the film, and finally pressing the ensemble together under about 2 MPa. The thickness of the CA layer on the electrode was about 150 μm. Electrochemical measurements (cyclic voltammetry (CV) and AC impedance) were carried out at room temperature using a 30% KOH aqueous solution as an electrolyte, and using an IM6e Electrochemical Workstation with a typical three-electrode configuration. The reference electrode is Ag/AgCl. In CV measurements, the potential scan rates were set as 0.5–100 mV/s. In AC impedance measurements, the range of frequency was set to go between 0.01 and 10000 Hz.

3. Results and discussion

3.1. Structural control and characterization of CAs

It is well known that the porous structures of CAs can be adjusted by gelation conditions and by activation [9,10]. We designed and controlled the porous structures of ACAs by mainly changing the R/C ratio, carbonization temperature and K/CA ratio, and we then characterized them by nitrogen adsorption and SEM. Figs. 1 and 2, respectively, show the pore size distribution of ACAs prepared with 125 and 500 R/C ratios and with different K/CA ratios. According to the curves of the pore size distribution (Figs. 1 and 2) and SEM observation (Fig. 3), we proposed a new porous model for CA materials. Different from the reported model in the literature [11], the new model divides the pores of CAs or ACAs into four types: (A) micropores with diameters below 2 nm, which are located within the carbon nanoparticles of the samples; (B) small mesopores with diameters from 2 to 5 nm, which are also located within the carbon nanoparticles; (C) large mesopores with diameters from 5 to 40 nm, which are formed from the closely packed carbon nanoparticles; (D) large pores and channels with diameters over 40 nm, which

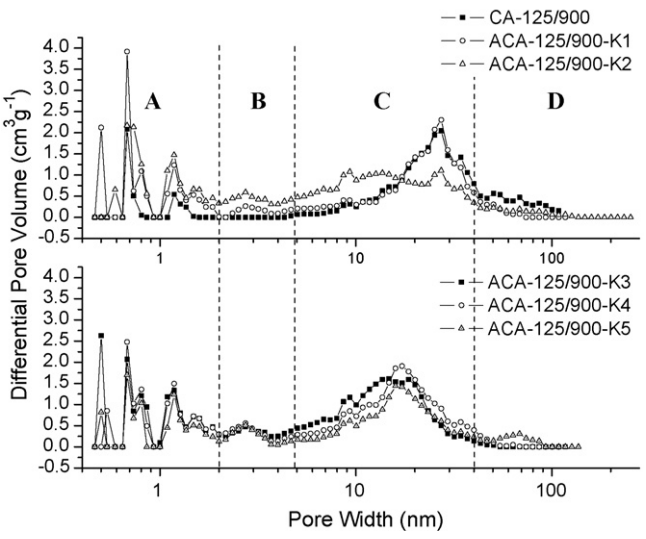

Fig. 1. Pore size distribution of ACA-125/900 samples with different K/CA ratios.

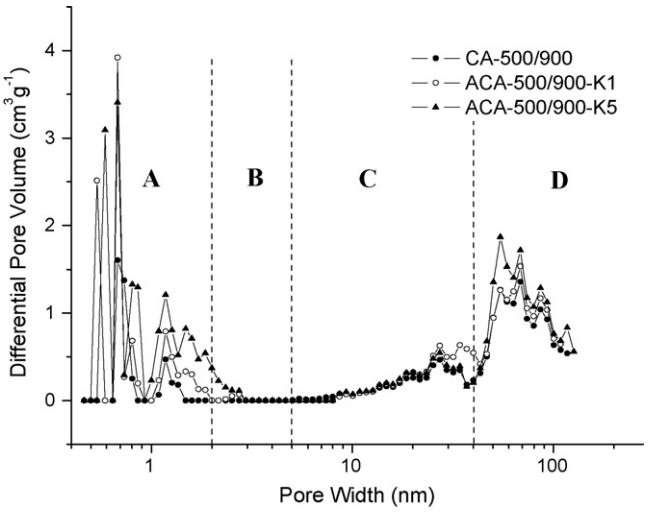

Fig. 2. Pore size distribution of ACA-500/900 samples with different K/CA ratios.

are formed from the loosely packed carbon nanoparticles. The pore model is schematically shown in Fig. 4. For the ACAs which were prepared, most of type A pores are interconnected with type B pores which are interconnected with type C or type D pores.

Generally, activation with KOH greatly increased the amount of type A pores and especially increased the number of type B pores, and sequentially increased the BET surface areas (see Figs. 1 and 2 and Table 1). However, when the CA was synthesized with a 125 R/C ratio, its network construction was weak and was easily damaged by KOH activation, which would cause the carbon nanoparticles to pack more closely. Therefore, the diameter of the type C pores of the ACA-125/900-K*z* materials was shifted down from 25 to 15 nm when the K/CA ratio increased from 1 to 5. When the K/CA ratio was over 5, the BET surface area of the ACAs would decrease.

However, the comparison of Figs. 1 and 2 indicated that an R/C ratio of 500 is advantageous to loosely pack the carbon nanoparticles and therefore these conditions obviously increase the amount of type D pores. Additionally, it can be seen from Fig. 2 that the diameters of the type C and D pores of the samples synthesized with the 500 R/C ratio were almost not affected by KOH activation because their network skeletons were strong and stable. Therefore, in order to increase the number of micropores and at the same time keep the number of large pores and channels unchanged, a value of 500 for the R/C ratio is recommended.

In order to reduce the concentration of KOH used for activation, which will benefit environmental protection, and to keep a high BET surface area for the ACAs, a semi-carbonization process (500 °C pre-carbonization) was adopted before impregnating the sample with KOH. The KOH solution was easily dispersed into the

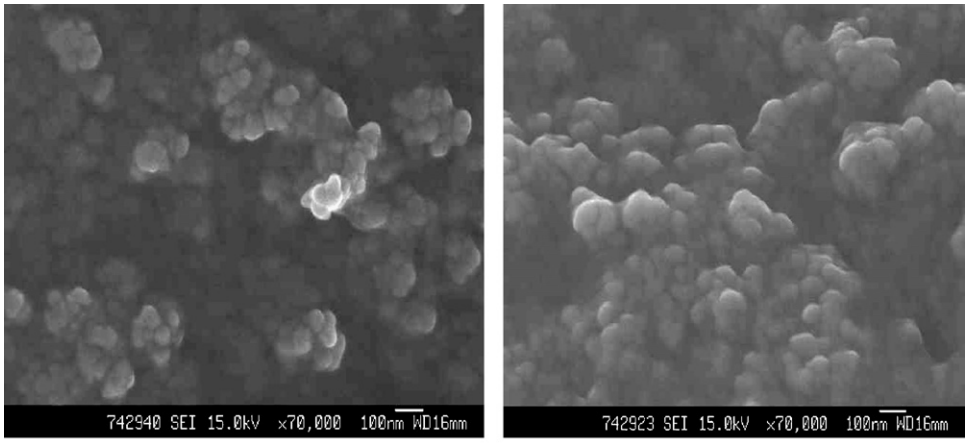

Fig. 3. SEM images of (A) CA-500/900 and (B) ACA-500/900-K5.

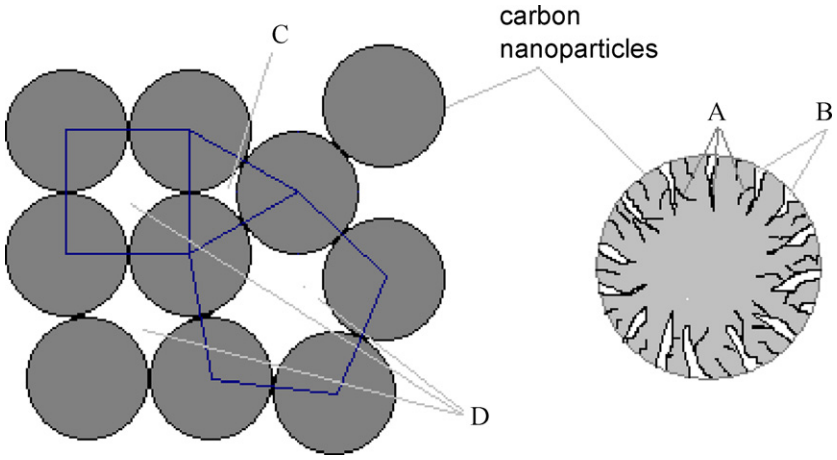

Fig. 4. Schematic diagram of pore structures of ACAs. (A) micropores within carbon nanoparticles; (B) small mesopores within carbon nanoparticles; (C) large mesopores formed from the closely packed carbon nanoparticles; (D) large pores and channels formed from the loosely packed carbon nanoparticles.

Table 1
Textual characteristics of the ACA-125/900 samples

Sample	S_{BET} ($m^2\ g^{-1}$)	S_{micro} ($m^2\ g^{-1}$)	S_{meso} ($m^2\ g^{-1}$)	V ($cm^3\ g^{-1}$)	V_{micro} ($cm^3\ g^{-1}$)	V_{meso} ($cm^3\ g^{-1}$)	PD_{BJH} (nm)
CA-125/900	607	326	310	1.29	0.15	1.17	15
ACA-125/900-K1	1374	751	617	1.68	0.35	1.35	8.7
ACA-125/900-K2	1591	715	873	1.70	0.33	1.40	6.4
ACA-125/900-K3	1626	741	868	1.74	0.34	1.42	6.5
ACA-125/900-K4	1628	647	969	1.92	0.29	1.65	6.8
ACA-125/900-K5	1268	361	867	1.70	0.16	1.55	7.1

Table 2
Specific capacitance (C_s) and equivalent series resistance (ESR) of ACAs

Sample	S_{BET} ($m^2\ g^{-1}$)	C_s ($F\ g^{-1}$)			ESR_1 (Ω) at 10 kHz	ESR_2 (Ω) at 10 mHz
		10 mV/s	50 mV/s	100 mV/s		
CA-125/900	607	101	84	72	0.2	12.6
ACA-125/900-K1	1374	147	119	96	0.42	11.1
ACA-125/900-K3	1626	143	119	97	0.78	11.8
ACA-125/900-K5	1268	78	71	60	0.21	22.0
CA-500/900	520	107	83	66	0.16	18.2
ACA-500/900-K1	997	173	145	130	0.37	11.6
ACA-500/900-K5	1619	199	182	170	0.17	15.2
ACA-500/500-K1	1468	245	217	201	0.80	17.2
ACA-500/500-K7	3247	244	149	100	0.89	37.6

semi-carbonized aerogel samples because the density of the aerogel matrix is lower than that of the fully carbonized particles. On the other hand, the semi-carbonized matrix was also active and easily etched by KOH. Therefore, though the K/CA ratio was 1, the BET surface area of the ACA-500/500-K1 was as high as 1468 $m^2\ g^{-1}$ (Table 2). When the K/CA ratio was at 3 or 7, the BET surface area of the ACA-500/500-Kz was over 2000, or as high as 3247 $m^2\ g^{-1}$. For high concentration KOH activation, the small mesopores (type B) of the semi-carbonized ACAs also obviously increased (Fig. 5). But it must be pointed out that the network structure of the ACAs in this case was badly damaged and collapsed according to the SEM observation (Fig. 6), and therefore the large pores and channels (type D pores) disappeared from the samples (see Fig. 5).

3.2. Effect of porous structures on electrochemical performance

When the ACAs thus prepared were used as electrodes, they presented perfect rectangular voltammograms (Fig. 7) [6]. Table 2 shows the specific capacitance (C_s) and equivalent series resistance (ESR) of ACAs. It can be seen that KOH activation obviously increases the C_s of the ACAs. The highest C_s of the ACAs reached 245 $F\ g^{-1}$ at 10 mV/s, which is higher than that of commercial super-activated

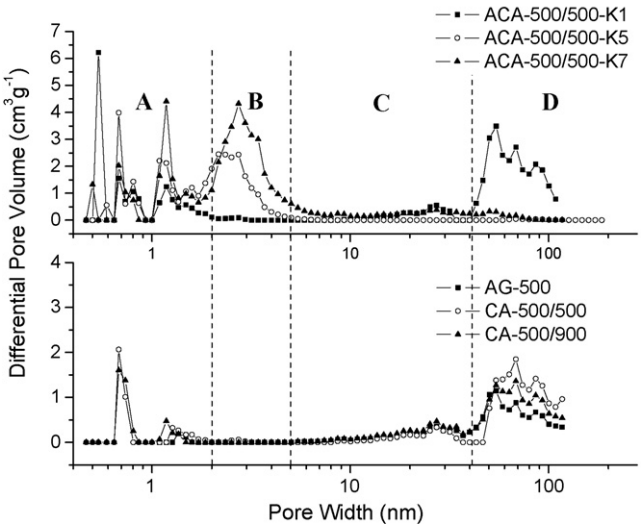

Fig. 5. Pore size distribution of various samples (see text).

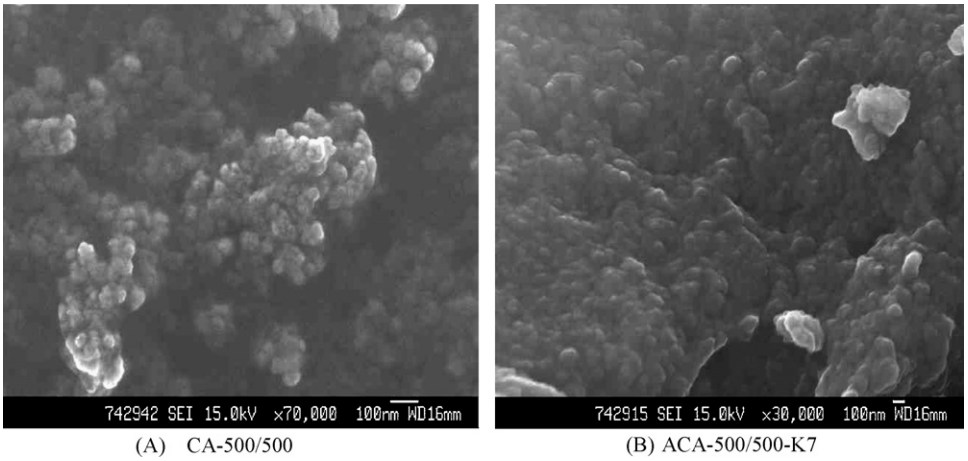

(A) CA-500/500 (B) ACA-500/500-K7

Fig. 6. SEM images of (A) CA-500/500 and (B) ACA-500/500-K7.

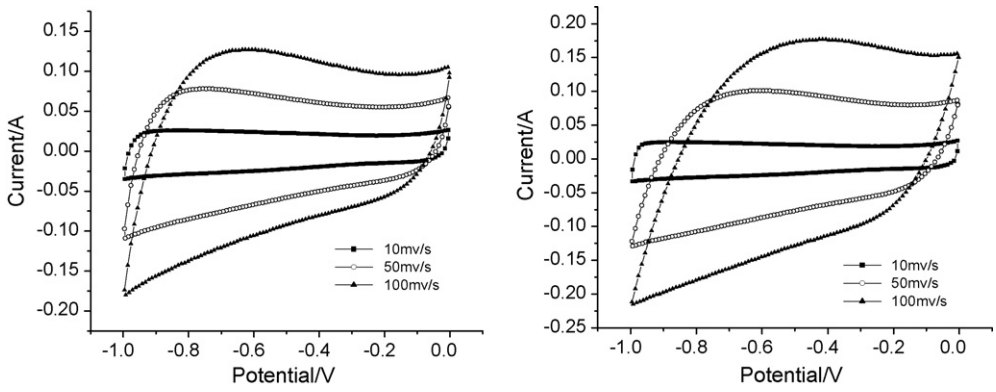

Fig. 7. Cyclic voltammetry of the electrodes of the CA-500/900 (Left) and ACA-500/900-K1 (Right) samples.

carbon (HNAC-1, 232 F g^{-1} at 10 mV/s) under the same measurement conditions. However, violent activation resulting from a high concentration of KOH (high K/CA ratio) might increase the BET area of the aerogel samples but not the C_s because violent activation would damage the relevant large pores and the channels of the samples. Therefore, ACA-500/500-K1 has the highest C_s, due to its appropriate high BET areas, as well as large pores and channels. It is very important to emphasize that this sample also shows a high-speed charge–discharge performance. Its C_s at 100 mV/s was as high as 201 F g^{-1}, which was 82% of the value at 10 mV/s. It is suggested that the high-speed charge–discharge performance of the ACA-500/500-K1 is attributed to the abundant type D pores, which play an important role in the transfer of the electrolyte. When the samples were activated with a high concentration of KOH that caused the collapse of the large pores, such as for the samples ACA-125/900-K5 and ACA-500/500-K7, their capacitances would greatly decrease, or their capacitances under high charge–discharge currents obviously decreased (see Table 2) because of the collapse of the type D pores (see Fig. 5). These results indicated that the type D pores of the ACAs are very useful for charge–discharge propagation.

According to their pores, we divided the ACAs into two groups (see Fig. 8). Group I includes the samples that mainly contain type A, type B and type D pores; Group II includes those mainly containing type A, type B and small diameter C pores. We found that both groups of carbons show a linear relation between the C_s and the BET area, separately (Fig. 9) [5,6]. But the slope of the linear line for Group I samples ($C_s = 0.14S_{BET} + 36.5$) is much higher than that for Group II samples ($C_s = 0.058S_{BET} + 46.9$). That is, the surface area (or micropores) of Group I samples are more efficiently used in the storage of energy.

In addition, the effect of the pore distribution on the electrochemical performance can also be seen from Figs. 10 and 11. The impedances and capacitances of Group II samples decrease more quickly than those of Group I with an increase in the detection frequency.

Considering together the porous structures and the electrochemical performance of the Group I and Group II samples that were prepared, it is suggested that the micropores of the ACAs (type A pore) play an essential role for the accumulation of charges, so that Group I and Group II ACAs both showed a linear relation between the C_s and the BET area, separately. However, the micropores must be electrochemically accessible for ions to establish the electrical double layer [6]. The micropores in Group II ACAs are poorly accessible because they are blocked by the much more tightly packed carbon nanoparticles (forming closed type C pores with small diameter). The abundant type D pores in Group I ACAs provide a rapid mass transport of ions within the electrode, facilitating the charging and discharging of the double layer. Therefore, the porous structure of the abundant type D pores which are interconnected with small mesopores, which in turn, are interconnected with micropores is very important for enhancing the efficient electrochemical surface area and increasing the

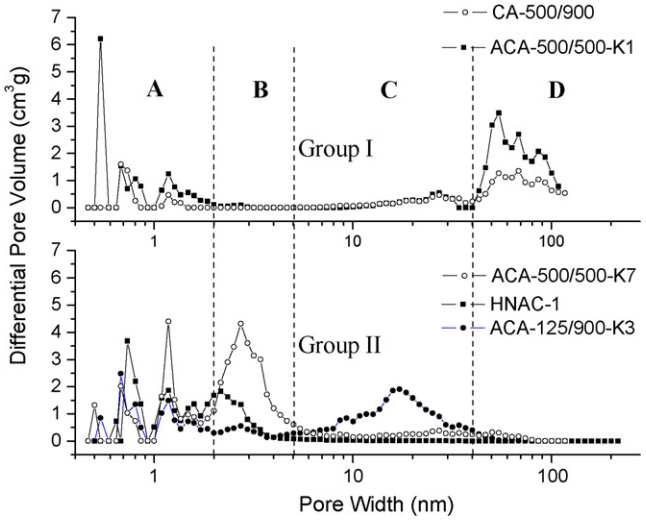

Fig. 8. Pore size distribution of porous carbon samples discussed in the text.

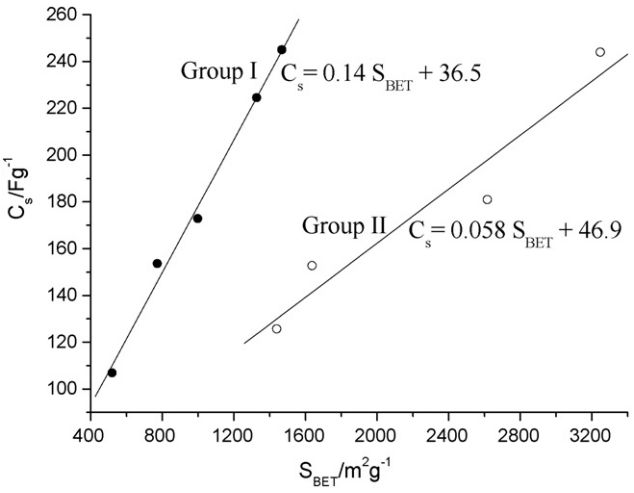

Fig. 9. Linear relationship between C_s and the BET area of Group I and Group II ACAs (see text).

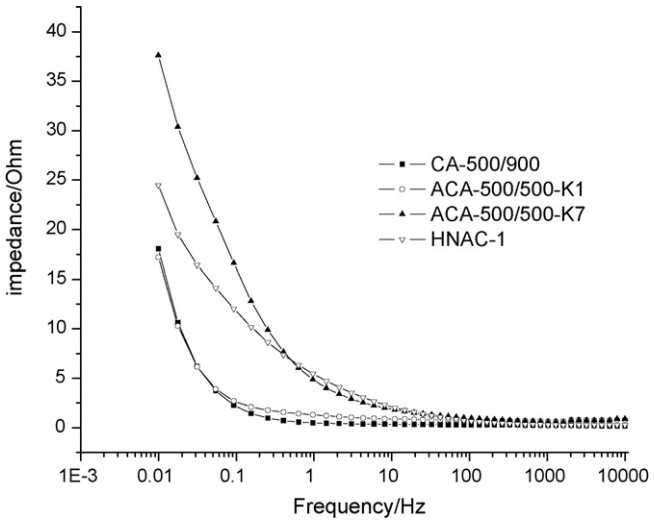

Fig. 10. Impedance–frequency curves for different samples (see text).

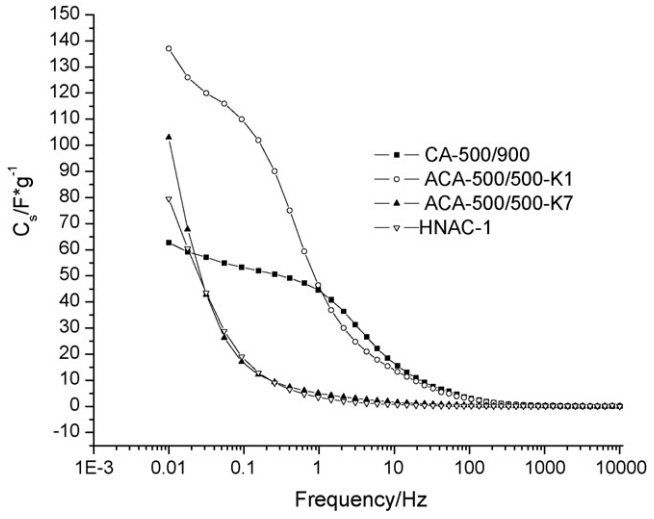

Fig. 11. Capacitance–frequency curves for different samples (see text).

accessibility of micropores. This enhancement in surface area and increase in accessibility greatly increase the electrochemical capacitance of the ACAs produced under high charge–discharge current conditions.

4. Conclusions

A new porous model for CA materials is proposed, in which the pores of the ACAs that were prepared are divided into four types: (A) micropores with diameters below 2 nm; (B) small mesopores with diameters from 2 to 5 nm; (C) large mesopores with diameters from 5 to 40 nm; and (D) large pores and channels with diameters over 40 nm. Appropriate activation with KOH increased both the number of type A pores and the BET areas, which in turn increased their C_s. The type D large pores and channels formed from the loosely packed carbon nanoparticles played an important role in the transfer of the electrolyte, which greatly increased the electrochemical capacitance under high charge–discharge current conditions. Violent activation with a high concentration of KOH might damage the relevant large pores and the channels which obviously decreased the electrochemical capacitance and rapid charge–discharge performance. Though the ACAs with different porous models exhibited a linear relation between the C_s and BET area separately, the surface area (or micropores) of the ACAs with appropriate large pores and channels (type D pores) were more efficiently used in the storage of energy than those with closed type C pores.

Acknowledgements

This research was supported by the Project of NNSFC (50472029 and 50632040), the Scientific Foundation of Guangdong (2004A30404001), and the Scientific Foundation of Guangzhou (2007Z2-D2041). M. S. Dresselhaus and G. Dresselhaus acknowledge support from NSF/DMR 07-04197.

References

[1] E. Frackowiak, F. Beguin, Carbon 39 (2001) 937–950.
[2] R.W. Pekala, J.C. Farmer, C.T. Alviso, T.D. Tran, S.T. Mayer, J.M. Miller, B. Dunn, J. Non-Cryst. Solids 225 (1998) 74–80.
[3] C. Schmit, H. Probstle, J. Fricke, J. Non-Cryst. Solids 285 (2001) 277–282.
[4] R. Saliger, U. Fischer, C. Herta, J. Fricke, J. Non-Cryst. Solids 225 (1998) 81–85.
[5] Q.H. Meng, L. Liu, H.H. Song, R. Zhang, L.C. Ling, J. Inorg. Mater. 19 (2004) 593–598.
[6] E. Frackowiak, Phys. Chem. Chem. Phys. 9 (2007) 1774–1785.
[7] P. Azais, L. Duclaux, P. Florian, D. Massiot, M.A. Lillo-Rodenas, A. Linares-Solano, J.P. Peres, C. Jehoulet, F. Beguin, J. Power Sources 171 (2007) 1046–1053.
[8] X.G. Zhuang, Y.S. Yang, Y.J. Ji, D.P. Yang, Z.Y. Tang, ACTA Phys.-Chem. Sin. 19 (2003) 689–694.
[9] D. Wu, R. Fu, M.S. Dresselhaus, G. Dresselhaus, Carbon 44 (2006) 675–681.
[10] Y. Hanzawa, K. Kaneko, R.W. Pekala, M.S. Dresselhaus, Langmuir 12 (1996) 6167–6169.
[11] A.W.P. Fung, Z.H. Wang, K. Lu, M.S. Dresselhaus, R.W. Pekala, J. Mater. Res. 8 (1993) 1875–1885.